PHYSICAL REVIEW B VOLUME 35, NUMBER 4 1 FEBRUARY 1987

Multiple-quantum-flux penetration in a superconducting loop containing a Josephson junction: Temperature dependence

James A. Blackburn
Department of Physics and Computing, Wilfrid Laurier University, Waterloo, Ontario, Canada

H. J. T. Smith
Department of Physics, University of Waterloo, Waterloo, Ontario, Canada
(Received 17 July 1986)

A temperature-dependent resistivity shunted junction (RSJ) model with a piecewise linear quasiparticle characteristic has been used in simulations to predict the flux dynamics in a superconducting ring containing a single Josephson junction. The computed results for relative flux penetration do not agree well with experimental data at temperatures approaching T_c. This indicates either that the subgap damping is not directly deducible from junction tunneling characteristics, or that the RSJ model is not sufficiently general in this situation.

I. INTRODUCTION

The arrangement of a superconducting ring interrupted by one or more Josephson junctions is of considerable importance, particularly because it is the central element in superconducting quantum interference devices (SQUID's). An extensive literature now exists detailing the dynamical behavior of such systems.

Our interest in this problem began with a consideration of flux entry into a magnetic-field-biased loop.[1] For a sufficiently large applied field, a number of flux quanta will pass through the Josephson junction and into the interior of the ring. It was discovered that this number was a universal function of the junction damping parameter. Wang and Gayley[2] extended this work to regions of low damping, while Peterson and Gayley[3] considered the implications of the $\cos\phi$ conductance term. The extension to N junctions in a ring was examined by Yamashita *et al.*[4] and Blackburn.[5] The flux dynamics in a double-junction interferometer were studied by Blackburn and Smith.[6] A slightly different topological configuration involving two parallel junctions in a ring was also considered.[7]

The vast majority of computer simulations of systems involving the time-dependent properties of Josephson junctions employ the resistivity shunted junction (RSJ) model[8] with *constant* shunt resistance. This condition is, for example, utilized in Refs. 1–8. The observed current-voltage characteristic of a Josephson tunnel junction with capacitance is, however, decidedly nonlinear. Above the energy gap, a normal resistance R_N is observed. Below the gap the I-V curve is generally both temperature and voltage dependent. Thus the conventional RSJ model with fixed resistance is at best an approximation, although it appears to give satisfactory results in many situations. Nevertheless it cannot reproduce any behavior associated with the energy gap, which it implicitly ignores.

An obvious improvement is achieved by employing a voltage-dependent quasiparticle resistance in the RSJ equivalent circuit for the Josephson junction. Scott[9] used experimental quasiparticle tunneling data to compute theoretical I-V characteristics for Josephson junctions and obtained good agreement for the temperature-dependent hysteresis. A similar approach was taken by Gayley[10] in simulation studies of switching to the finite voltage state of a current-biased Josephson junction. In that work calculations were also carried out using a formalism based on the full Bardeen-Cooper-Schrieffer (BCS) theory. Piecewise linear approximations for $R(V)$ have been employed by Zappe,[11] Ben-Jacob and Imry,[12] Smith and Jillie,[13] and Iansiti *et al.*[14] in connection with laser irradiated junctions.

In this paper we generalize our original work[1] by taking account of the difference in the quasiparticle resistance when the junction voltage is either above or below the gap value. Particular attention is paid to the modified RSJ model with respect to behavior *at the gap voltage* where, for finite intervals of time, the effective resistance depends on the junction current rather than voltage (which is temporarily clamped). The known temperature dependence of the subgap resistance is then used to predict resulting variations in the flux entry dynamics. Finally, we discuss these simulation results in relation to experimental data obtained from a relatively large inductance ring containing a thin-film Josephson junction.

II. THEORY

Consider a superconducting ring of inductance L which is interrupted by a Josephson junction having capacitance C, maximum supercurrent i_c, normal resistance (above the gap) R_N, and a subgap quasiparticle resistance R_{qp}. We follow a convention used previously[5] in which, by a right-hand rule, flux (ϕ) is positive up, and phase (θ) and current (i) are positive counterclockwise. Then the total loop current is given by

$$i = i_c \sin\theta + \frac{\hbar\dot{\theta}}{2eR} + \frac{\hbar C}{2e}\ddot{\theta} . \tag{1}$$

Dots indicate time derivatives.

The net flux contained in the loop is related to the junction phase

$$\theta = -2\pi(\phi/\phi_0) , \tag{2}$$

where ϕ_0 is the flux quantum. Finally, we have

$$\phi = \phi_x + Li , \tag{3}$$

where ϕ_x is the externally applied bias flux. Combining (1)—(3), normalizing flux by ϕ_0, and measuring time in units of $\sqrt{LC}$, we obtain the following differential equation:

$$\Phi'' + \frac{1}{R}\sqrt{L/C}\,\Phi' + \frac{Li_c}{\phi_0}\sin(2\pi\Phi) = \Phi_x - \Phi . \tag{4}$$

Primes indicate derivates with respect to dimensionless time. Using the usual Josephson relation for junction voltage, $\dot{\theta} = 2eV/\hbar$ and the connection between gap parameter Δ and gap voltage $V_g (= 2\Delta/e)$, we find for the dimensionless flux velocity corresponding to the gap voltage

$$(\Phi')_g = 2\sqrt{LC}/\tau ,$$

where τ is the gap response time, $h/2\Delta$. Gayley[10,15] introduced a parameter $\alpha \equiv R_N C/\tau$ to characterize the switching speed of Josephson junctions. We define $\beta_0 \equiv (1/R_N)\sqrt{L/C}$, which is the damping above the gap, and $\gamma \equiv Li_c/\phi_0$. Then

$$(\Phi')_g = 2\alpha\beta_0 \tag{5}$$

and the differential equation (4) becomes

$$\Phi'' + \beta\Phi' + \gamma\sin(2\pi\Phi) = \Phi_x - \Phi , \tag{6}$$

where $\beta \equiv (1/R)\sqrt{L/C}$ is equal to β_0 above the gap ($\Phi' > 2\alpha\beta_0$) and is $\mathscr{R}\beta_0$ below the gap ($\Phi' < 2\alpha\beta_0$), with $\mathscr{R} \equiv R_N/R_{qp}$.

The assumed current-voltage characteristic is shown in Fig. 1; it consists of two linear segments connected at the gap voltage. The corner points occur at currents i_1 and i_2. From this diagram it is apparent that $i_1 = V_g/R_{qp}$ and $i_2 = V_g/R_N$. It is then possible to show from these expressions that

$$i_1/i_c = 2\alpha\beta_0^2\mathscr{R}/\gamma , \tag{7}$$

$$i_2/i_c = 2\alpha\beta_0^2/\gamma . \tag{8}$$

The problem has now been completely specified in terms of four dimensionless parameters: α, β_0, γ, and $\mathscr{R}$. In our earlier study which assumed constant damping, only two parameters appeared: β_0 and γ.

The three current components flowing in the Josephson junction are the supercurrent $i_c\sin\theta$, the normal current V/R, and the displacement current $C\,dV/dt$. If these are normalized to the critical supercurrent i_c and converted to dimensionless flux and its derivatives, we obtain

$$I_J = -\sin(2\pi\Phi) , \tag{9}$$

$$I_R = -(\beta/\gamma)\Phi' , \tag{10}$$

$$I_C = -(1/\gamma)\Phi'' . \tag{11}$$

The total loop current I is just the sum $I_J + I_R + I_C$.

We wish to examine the temperature dependence of the flux dynamics in this system. To do so we must model the related variations $\alpha(T)$, $\gamma(T)$, and $\mathscr{R}(T)$. The source of these dependences lies in the functions $\Delta(T)$ and $i_c(T)$. Clearly $\alpha(T/T_c)$ has the same functional form as $\Delta(T/T_c)$, whereas $\gamma(T/T_c)$ varies as $i_c(T/T_c)$. We will treat $\mathscr{R}(T/T_c)$ as a function to be determined.

It is a well-known property at $T = 0$ that the point $[(\pi/4)V_g, i_c]$ lies on the normal resistance line extended to the origin. By simple geometry applied to Fig. 1 it can be seen that $i_2/i_c = 4/\pi$. Combining this expression with Eq. (8), we obtain

$$\alpha = \frac{2\gamma}{\pi\beta_0^2} \quad \text{at } T = 0 . \tag{12}$$

This result has also been noted by Gayley.[15] Thus we see that choosing any two of $(\alpha, \beta_0, \gamma)$ immediately fixes the third at $T = 0$. When we compute the flux entry properties for the loop, it will be sufficient to classify the results according to the value of $\alpha(T = 0)$ and the assumed form for $\mathscr{R}(T/T_c)$. This parametrization in the ratio γ/β_0^2 is significant in that it was found previously[1,3] that the relative number of flux quanta which entered a ring, Φ_e/γ, was a universal function of β/β_c, where $\beta = \beta_0$ in the present notation, and $\beta_c \simeq 3\sqrt{\gamma}$. In other words $\alpha(T = 0)$ is proportional to $(\beta_c/\beta_0)^2$.

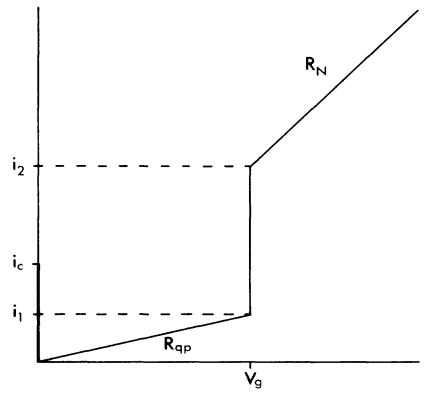

FIG. 1. Piecewise linear I-V characteristic for a tunnel junction. The voltage at the superconducting energy gap is V_g. Corner points for the vertical segment occur at i_1 and i_2. The maximum Josephson supercurrent is i_c.

III. SIMULATION RESULTS

The results presented here were computed in double-precision arithmetic on a time grid with $\Delta t = 0.000\,02$. The scheme by which numerical solutions were obtained is summarized in Table I. When the junction operating point is moving along the I-V characteristic above (R_N) or below (R_{qp}) the gap, the differential equation is solved with a fourth-order Runge-Kutta routine. However, when the gap is reached from either resistive segment, the vertical portion of the characteristic must then be followed. This takes place at constant voltage and so $\Phi'' = 0$. The

TABLE I. Summary of procedures followed in solving the equation of motion for the loop flux.

(1) $V<V_g$ $\Phi'<2\alpha\beta_0$	(2) $V>V_g$ $\Phi'>2\alpha\beta_0$	(3) $V=V_g$ $\Phi'=2\alpha\beta_0$
$\beta=\mathscr{R}\beta_0$	$\beta=\beta_0$	
$\Phi''=-\beta\Phi'-\gamma\sin(2\pi\Phi)-\Phi+\Phi_x$		$\Phi(t)=\Phi(t-\Delta t)+2\alpha\beta_0\Delta t$
Solve by Runge-Kutta routine		
$I_J=-\sin(2\pi\Phi)$		$I_J=-\sin(2\pi\Phi)$
$I_C=-\Phi''/\gamma$		$I_C=0$
$I_R=-\Phi'(\beta/\gamma)$		$I=(\Phi-\Phi_x)/\gamma$
$I=I_J+I_C+I_R$		$I_R=I-(I_J+I_C)$
Test		Tests
$V=V_g$: Go to (3)		$I_R<2\alpha\beta_0^2\mathscr{R}/\gamma$: Go to (1)
		$I_R>2\alpha\beta_0^2/\gamma$: Go to (2)

sequence of calculations appropriate to this situation is also shown in the table. Transfer to and from the gap segment are governed by the indicated test conditions.

Although other authors[10,12,13,14] have carried out computations with voltage-dependent resistance, procedural details were not provided on the important role played by the vertical segment at the gap. As we shall see, the junction can spend an appreciable amount of time in each cycle locked at V_g.

A typical plot of flux velocity versus time is presented in Fig. 2(a). The external flux Φ_x was initially set to zero and was then linearly ramped up to a value of $\gamma+0.5$ in

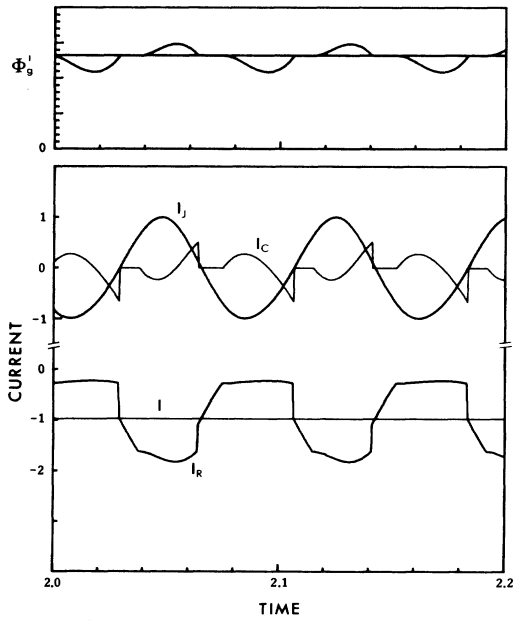

FIG. 2. (a) Portion of $\Phi'(t)$ for $T/T_c=0.7$ and $\beta_0=80$. At this temperature, $\alpha=0.0825$, $\gamma=650$, and $\mathscr{R}=0.172$. Apart from a scale factor, this also is equivalent to a plot of junction voltage with the horizontal reference line corresponding to the energy gap. (b) Time dependence of the total loop current and its components flowing through the junction circuit elements.

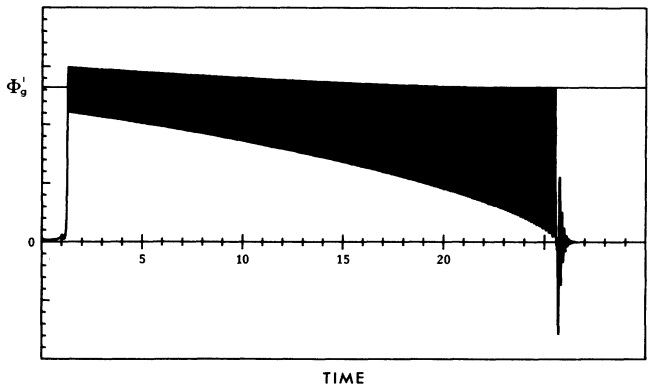

FIG. 3. Entire $\Phi'(t)$ pulse with parameter values as in Fig. 2. Because of the time scale, individual oscillations cannot be distinguished. A total of 263 flux quanta enter the ring before the damped plasma oscillations terminate the process. Note that the corresponding voltage pulse tends to be clamped from above at the gap value.

one time unit. The flux velocity corresponding to the gap voltage was determined from Eq. (5). The parameters indicated are appropriate to $T/T_c=0.7$; they originate from values of $\alpha=0.0995$ and $\gamma=1000$ at $T=0$. From Eq. (12) we then require $\beta_0=80$. Rescaling of α and γ was performed with the aid of the known temperature dependence of Δ (Ref. 16) and i_c (Ref. 17) for tin-oxide-tin tunnel junctions. The corresponding current components are shown in Fig. 2(b). As expected, the current through the capacitive element shuts off during the voltage clamping intervals. Note, however, that the *total* loop current exhibits a slow monotonic decay (it appears to be nearly constant on this greatly expanded time scale).

A plot of the entire $\Phi'(t)$ waveform is shown in Fig. 3. In this example a total of 263 flux quanta entered the loop before the process terminated with damped plasma oscillations whose period, in normalized units, is $\sqrt{2\pi/\gamma}$.

Below the gap actual I-V characteristics are highly nonlinear, whereas our assumed $I(V)$, as shown in Fig. 1, is a simplified function. We approximated R_{qp} from experimental data for a weak-coupling superconductor[18] by linearizing the subgap portion of the characteristic. The resulting temperature dependence of $\mathscr{R}$ is shown in Fig. 4(a).

In Fig. 4(b) we plot Φ_e/γ as a function of reduced temperature. Computations were performed with $\gamma(0)=1000$ or 500, and $\beta_0=[2\gamma(0)/\pi\alpha(0)]^{1/2}$, as required by Eq. (12). Each of the curves is fully characterized by its value of α at $T/T_c=0$. At low temperatures the quasiparticle current below the gap is small; hence R_{qp} is large and the associated damping is light. Therefore the dominant contribution to the overall damping comes from motion above V_g, when $\beta=\beta_0$. Because $\beta_0/\beta_c\simeq\frac{1}{3}\sqrt{2/\pi\alpha(0)}$ it is clear, for example, that small $\alpha(0)$ corresponds to heavy damping with resulting low relative flux penetration. This explains the general nested configuration of the Φ_e/γ curves.

With increasing temperature the subgap damping increases towards the value β_0. At the same time, however, $\gamma(T/T_c)$ decreases because of its dependence on i_c. Thus

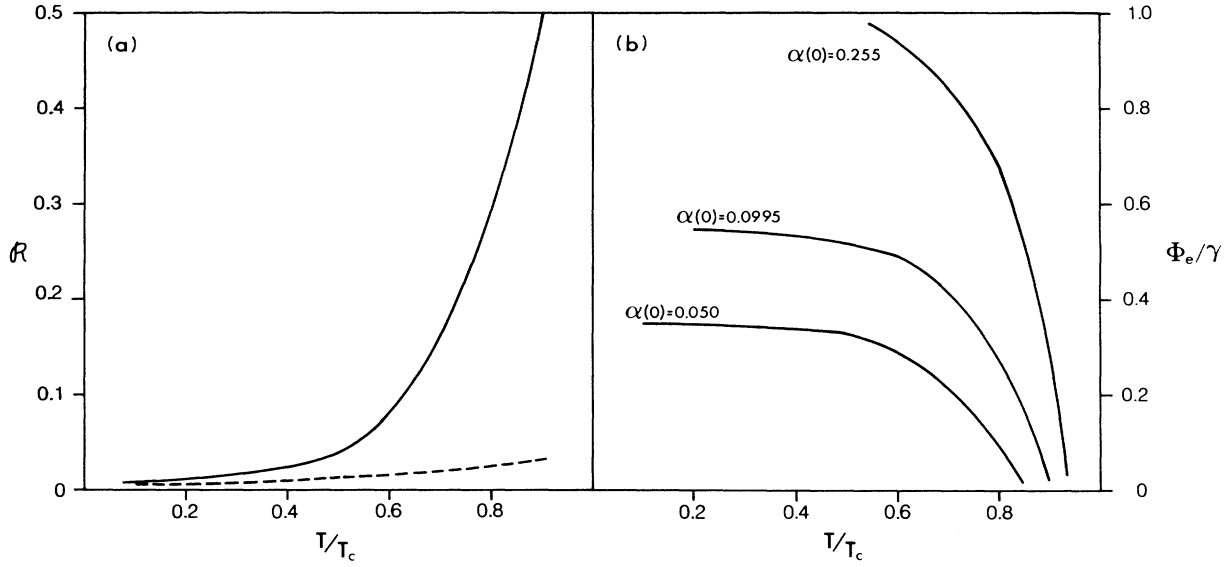

FIG. 4. (a) Approximate resistance ratio $\mathscr{R}$ as a function of reduced temperature for tin-oxide-tin tunnel junctions. The dashed curve represents an $\mathscr{R}(T/T_c)$ dependence which yields constant $\Phi_e/\gamma=0.35$. (b) Relative number of flux quanta entering the loop as a function of reduced temperature. These simulation results assume the resistance ratio shown in (a).

as the overall damping grows, the critical damping, which is proportional to $\sqrt{\gamma}$, decreases. Consequently, both factors force the ratio β/β_c towards unity at some particular temperature. This explains the rapid rolloff of Φ_e/γ with increasing T/T_c.

Experimental data (to be discussed in the next section) do not exhibit such a rolloff. Instead we found that the relative number of flux quanta which penetrated the loop was nearly independent of temperature. This led us to ask: What form of $\mathscr{R}(T/T_c)$ would result in a nearly constant Φ_e/γ? The answer is shown in Fig. 4(a); this assumed resistance ratio yields $\Phi_e/\gamma=0.35$ for $0.1\leq T/T_c\leq 0.9$.

IV. EXPERIMENTAL RESULTS AND DISCUSSION

The apparatus employed for this study has been described elsewhere.[1] Briefly, it consisted of a superconducting ring of inductance $\sim 10^{-6}$ H into which is inserted an evaporated film tin-oxide-tin Josephson junction. The parameter γ was very large ($\sim 10^5$)—a consequence of the relatively high loop inductance. The junction capacitance was estimated to be approximately 10^{-12} F. A bias field ϕ_x was supplied by Helmholtz coils and the total circulating ring current was detected by a flux gate magnetometer.

As the applied field was slowly increased in magnitude, the loop current was observed to rise linearly until the maximum Josephson supercurrent was reached. When this occurred, bundles of flux quanta rapidly entered the ring through the junction and the circulating current abruptly decreased. The proportional drop in current is just Φ_e/γ.

Figure 5 displays typical results for the relative flux penetration as a function of reduced temperature. It is significant that very little rolloff is observed even near $T/T_c=1.0$. Simulations yield such behavior only when the resistance ratio remains small throughout the temperature range; this was noted in connection with Fig. 4(a). This conclusion that the damping below the gap remains relatively light is supported by an earlier study of self-resonance in a Josephson junction. These experiments[19] demonstrated that the resonant peaks had higher Q values than would be assumed from the quasiparticle characteristics.

Hence it appears that, with respect to a piecewise linear RSJ model, the subgap damping is more weakly temperature dependent than would be deduced from standard tunneling measurements.[18,20] The failure of the resistively shunted junction model to predict the observed behavior of Φ_e/γ is not altogether surprising in view of the fact that this model is expected to be valid only when the rate of change of voltage is small compared to the gap fre-

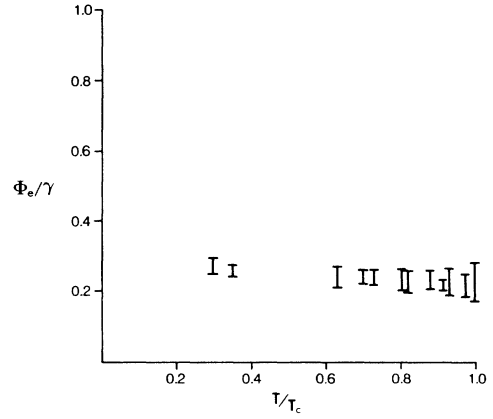

FIG. 5. Experimental results for tin-oxide-tin Josephson junction in a superconducting loop.

quency. In the present case we have seen (Figs. 2 and 3) that the junction spends an appreciable amount of time in the neighborhood of V_g. The damping thus arises from dynamical dissipation processes which are driven by the rapidly fluctuating junction voltage.

A more complete description of the junction which includes the frequency dependence of the complex supercurrent and quasiparticle components has been developed by Werthamer.[21] In a series of papers[22–24] Harris and others adapted this formalism to both voltage- and current-biased Josephson junctions. Subsequent work by Harris[25] and Gayley[10] considered the switching of a junction into the finite voltage state, and found that the RSJ model yielded results which were only qualitatively similar to those produced by the microscopically based theory. Such a conclusion was also reached by Peterson and McDonald[26] in an analysis of fast pulse generation in Josephson circuits.

As an additional comment, we observe that the RSJ model is of course highly simplified; indeed simplicity and ease of application are its chief virtues. By contrast the Harris-Werthamer approach is much more difficult to implement in circuit simulations. An intermediate formalism due to De Lustrac *et al.*[27] and based on a first-order series expansion of the tunneling current appears to offer an attractive compromise between microscopic completeness and the computational convenience of the RSJ model.

It is possible that these more general theoretical descriptions of a Josephson junction could yield better agreement with our experimental data at the higher reduced temperatures. We note in this regard that Gayley,[15] in numerical studies of a single-junction SQUID, found—for given β—that an RSJ calculation *underestimated* the relative amount of flux penetration (compared with the BCS result). The excess rolloff in our simulation curves (Fig. 4) might have a similar origin.

ACKNOWLEDGMENTS

This work was supported by grants from the Natural Science and Engineering Research Council of Canada.

[1]H. J. T. Smith and J. A. Blackburn, Phys. Rev. B **12**, 940 (1975).
[2]T. C. Wang and R. I. Gayley, Phys. Rev. B **15**, 3401 (1977).
[3]R. L. Peterson and R. I. Gayley, Phys. Rev. B **18**, 1198 (1978).
[4]T. Yamashita, Y. Ogawa, and Y. Onodera, J. Appl. Phys. **50**, 3547 (1979).
[5]J. A. Blackburn, J. Appl. Phys. **56**, 1477 (1984).
[6]J. A. Blackburn and H. J. T. Smith, J. Appl. Phys. **49**, 2452 (1978).
[7]J. A. Blackburn and H. J. T. Smith, J. Appl. Phys. **48**, 2961 (1977).
[8]D. E. McCumber, J. Appl. Phys. **39**, 3113 (1968).
[9]W. C. Scott, Appl. Phys. Lett. **17**, 166 (1970).
[10]R. I. Gayley, J. Appl. Phys. **52**, 1411 (1981).
[11]H. H. Zappe, J. Appl. Phys. **44**, 1371 (1973).
[12]E. Ben-Jacob and Y. Imry, J. Appl. Phys. **51**, 4317 (1980).
[13]L. N. Smith and D. W. Jillie, J. Appl. Phys. **52**, 5262 (1981).
[14]M. Iansiti, Qing Hu, R. M. Westervelt, and M. Tinkham, Phys. Rev. Lett. **55**, 746 (1985).
[15]R. I. Gayley, IEEE Trans. Mag. **MAG-17**, 809 (1981).
[16]L. Solymar, *Superconductive Tunnelling and Applications* (Wiley-Interscience, New York, 1972), Fig. 1.5, p. 17.
[17]A. Barone and G. Paterno, *Physics and Applications of the Josephson Effect* (Wiley-Interscience, New York, 1982), Fig. 3.2, p. 55.
[18]B. L. Blackford and R. H. March, Can J. Phys. **46**, 141 (1968).
[19]J. A. Blackburn, J. D. Leslie, and H. J. T. Smith, J. Appl. Phys. **42**, 1047 (1971).
[20]*Nonequilibrium Superconductivity, Phonons and Kapitza Boundaries,* edited by K. E. Gray (Plenum, New York, 1981), Chap. 5.
[21]N. R. Werthamer, Phys. Rev. **147**, 255 (1966).
[22]R. E. Harris, Phys. Rev. B **11**, 3329 (1975).
[23]D. G. McDonald, E. G. Johnson, and R. E. Harris, Phys. Rev. B **13**, 1028 (1976).
[24]R. E. Harris, Phys. Rev. B **13**, 3818 (1976).
[25]R. E. Harris, J. Appl. Phys. **48**, 5188 (1977).
[26]R. L. Peterson and D. G. McDonald, IEEE Trans. Mag. **MAG-13**, 887 (1977).
[27]A. De Lustrac, P. Crozat, and R. Adde, Rev. Phys. Appl. **21**, 319 (1986).